Transducers Science and Technology (EWI) Universiteit Twente

Bachelor Thesis Advanced Technology

Investigation of the mechanical properties of 3D printed structures of Objet and DLP.

Author:
Mathijs Schlepers
s1240544

Graduation committee:
Prof. dr. ir G.J.M. Krijnen
Prof. dr. ir. André de Boer
Dr. ir. T.H.J. Vaneker
Ing. R. Sanders

July 4, 2014 University of Twente

Abstract

The currunt solution for building transducers is done with MEMS technology (microelectromechanical systems). The building process is complex and generally takes a lot of time. It is therefore not possible to completely design and build a MEMS device at short notice. To increase the throughput of the process 3D printing might be used. This research is focussed on the investigation of the mechanical properties of 3D printed parts from Objet and DLP, printed as small as possible, in order to investigate the usability of 3D printed structures. Test structures designed in Solid Works were printed with Objet and DLP printers. These designs were characterised with respect to minimum block size, accuracy, Young's Modulus and Shear Modulus of the printed structures. The minimum block size and accuracy are measured with an optical microscope. The Young's Modulus is measured dynamically and statically and the Shear Modulus only statically. It was possible to measure all quantities. Only the dynamically and statically measured Young's Modulus results showed large deviations. This was due to a large error made in the static measurements. The minimum block size ranges between 150μm and 500μm for DLP and 250μm and 300μm for Objet printed structures. The accuracy achieved for the DLP was the best in the xy-plane. The accuracy for the Objet printer was approximately the same in all planes due to the use of support material. The Young's Modulus and Shear Modulus of the Objet printed items where max 2.5$\pm$0.15 GPa and 0.24$\pm$0.018 GPa and for the DLP 1.1$\pm$0.06 GPa and 0.012$\pm$0.001 GPa. Also some anisotropy was observed; the Young's Modulus was the highest in the xy-plane and the smallest in the z direction. With those indicated Young's Modulus and Shear Modulus known it is possible to design transducers. The minimum block size and accuracy are still to high to reach the same accuracy as MEMS technology, however it is possible to build transducers at an bigger size, furthermore it is possible to increase the manufacturing process of transducers with 3D print technolgy.

Contents

1 Introduction and research goals

1.1 Introduction

3D printing is a technique in which a structure is fabricated by printing it slice by slice. A digital model designed with CAD is cut into layers with preset separation distances and printed layer after layer. This process makes it possible to rapidly build structures, 3D printing is also called rapid prototyping or additive manufacturing. There have been great interest in the possibility to use 3D printing technology in the fabrication of transducers, because traditional MEMS designing and fabrication generally takes a lot of time. The droughput might be accelerated with the use of 3D printing. This thesis investigate if it is possible to build transducers with 3D print technology. Designs of transducers require detailed information about material parameters such as the stiffness and Shear Modulus. Therefore there is a need for information on the mechanical properties, but also on minimum block or hole size and print accuracy to know how small can be printed. Two accurate printing technologies are used and compared: The Objet and Digital light processing. These printers will be used to fabricate the test structures which will be analyzed in this thesis to determine the indicated properties.

1.2 Research goals

The research will focus on finding the mechanical properties of 3D printed structures from Objet and DLP print technologies. The first step will focus on estimating the minimum block or hole size and the accuracy of the two printers. Those properties are investigated on all possible orientations Figure 13. This will give an estimation of the minimum printing size of the two technologies in order to verify if it can compete with MEMS technology. Second step is the investigation of the Youngs Modulus and Shear Modulus of the printed structures. Those properties will be analyzed in all orientations. This is executed in order to measure possible anisotropy of the material. Last step of the research will focus on the investigation of possible creep in the material due to tension.

2 Overview of commercially available 3D printing processes

2.1 What is 3D printing

3D printing, also called additive manufacturing, is a process of making a three dimensional real object of any shape from a digital model. 3D printing is actually just like regular 2D printing, but with an extra dimension added to it. This is done by cutting the virtual object in 2D slices and printing the real object slice by slice [1]. The slices (also called layers) are printed on top of each other and by adding slice after slice the volume of the object increases and the object slowly takes on the shape defined by the digital 3D model.

3D printing technology has already been around for more than 30 years. But it has only been widely available since a few years. Several 3D printing processes have been invented and developed since the late 1970s. The original printers were expensive, had limited capabilities and were large. Just like the first computers. The first 3D printer was developed by Chuck Hull of 3D Systems Corp in 1984. Today there are a large number of 3D printing processes available. They differ in the way the materials are put on and the number and properties of the materials that can be used.

3D printing technology is used for both manufacturing and prototyping. It is very suitable for prototyping, because the time it takes from idea to actual object is small. It is also easy to improve or change the product and print it again. The prototyping process becomes more transparent and improvements are made faster.

2.2 Material Extrusion

2.2.1 Fused Deposition Modeling (FDM)

FDM is based on drawing a pattern with a very precise hot glue gun. It works by extruding material through a nozzle to print one cross section of an object, followed by lowering the platform to repeat the process for a new layer. The nozzle of the printer contains resistive heaters which almost melt the plastic as it flows through the nozzle and forms a new layer. The extruded layer bonds to the layer below it and immediately hardens. This process is repeated several times till the object is finished. The FDM technology is common in less expensive printers and desktop 3D printers. The FDM method also uses a support material. This is used to support the part during printing. After the part is finished the support material has to be removed. This can be done ultrasonic cleaning in a water bath or by dissolving the support material. Holes or channels are possible to fabricate, but they have to be reachable from the outside to remove the support material. There may exist anisotropy in the material due to the additive layer method. The strength of the body is the weakest in the vertical build section [24]. Part shrinkage may occur and mostly in the X and Y direction of the object (where the Z direction is perpendicular to the

slices). Shrinkage occurs during the 2 steps of producing: the building step and the supports removing step. Generally, the FDM equipment software will compensate for shrinkage to ensure proper dimensions. Some typical properties of the FDM technology are shown in table 1.

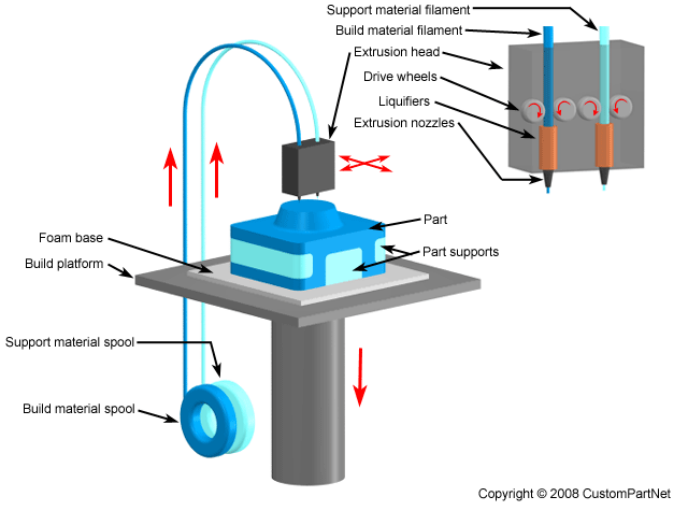

Figure 1: FDM principle [8]

Resolution	
Layer thickness	50-750 μm
Tolerances	>100 μm
Surface roughness	6-12 μm Ra
Supporting material	Yes
Channels possible	Yes

Table 1: Properties of FDM technology [24].

Materials used

The FDM printers are fed by so-called filaments, which are usually rolled on a spool. The materials are mainly thermoplastics or thermoplastic/organic blends. The most common materials used in FDM printing are Acrylonitrile butadiene styrene (ABS), polylactide (PLA) and polycarbonate (PC). The PLA is the most common used material, because it does not give nasty chemical fumes during printing and of its biodegradability. The next table represents the Youngs modulus and the Tensile strenght of ABS.

Material characteristics ABS	
Young's modulus	1400-3100 MPa
Tensile strenght	40MPa

Table 2: Material characteristics of ABS used in FMD printing [7].

Advantages

- The FDM printers are relative inexpensive.
- There are no toxic chemicals used, which makes it suitable for desktop use.
- Because of the supporting material the printer is able to print complex parts. For example overhaning beams.

Disadvantages

- The build speed is relatively slow.
- The surface finish is rough.
- Low resolution relative to other technologies.
- Support and build material are moderately expensive.

2.3 Vat photo polymerization

Vat photo polymerization is a sub group in 3D printing. Vat means a box which is filled with photopolymer.

2.3.1 Stereolithography

Charles W. Hull patented the method 'stereolithography' as a method and apparatus for building solid objects by printing thin layers [4]. The process uses a UV-laser and a basin with a photo sensitive solution in it. The platform is placed just under the liquid surface. When a UV beam hits the solution it solidifies locally through the process of photo polymerisation. The laser draws the cross section of the object causing the formation of a thin layer. After the layer is finished the platform descends by a distance equal to the thickness of a single layer. Subsequently the cross section of the object is re-coated with new material. Then the process starts again and the laser draws the cross section of the subsequent cross-section. A complete 3D part is build by this process. Finally the object is cured by placing it in an oven with ultraviolet light. Due to the layer by layer deposition the materials properties may be somewhat different in the direction perpendicular to the slices causing some anisotropy. The strength of the body is the weakest in the direction perpendicular to the cross-sections.

Holes or channels are possible only if one can access them from the outside.

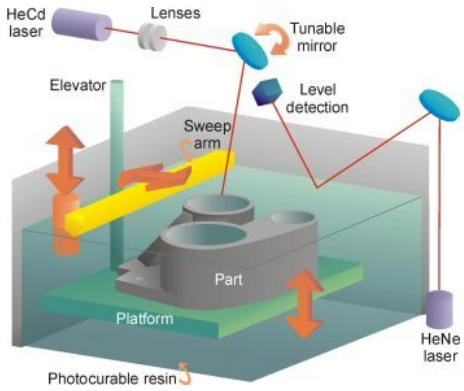

Figure 2: Stereolithography principle [20].

Resolution	
Layer thickness	25-150μm
Tolerances	>100μm
Surface roughness	2μm Ra
Supporting material	No
Channels possible	Yes

Table 3: Properties of Stereolithography [24].

Stereolithography necessitates the use of supporting structures which serve to attach the product to the elevator platform, hold it in place and prevent deflection due to gravity. The supports are generated automatically during the preparation with CAD. The supports must be removed manually, with a cutter or grinder after the product is finished. Part shrinkage occurs during the 3 steps of production: building, support removal and post-curing. The building distortion is caused due to layer-by-layer building. The lower layer suffers compression stress while the upper new hot layer suffers tension stress. This will cause the object to bend concave upwards Figure 3 . This is a problem for 3D printing technologies especially in stereolithography. After the build the supports are removed thereby partly releasing residual stresses, the object will settle to a new equilibrium state of internal stresses. At the last step the object is post cured in an oven with ultraviolet light. Exposure to the UV light cures and soldifies the structure. This will result in larger deviations of the dimensions. The stereolithography software will make corrections to compensate for the various causes of shrink to ensure right dimensions.

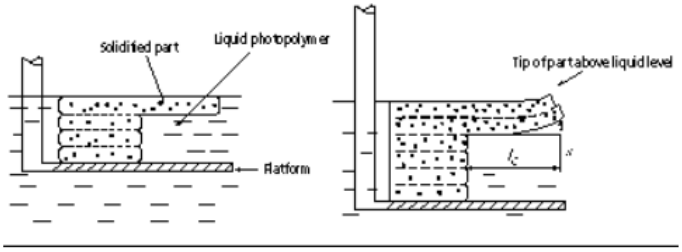

Figure 3: Principle of curl [14]. .

Materials used

Stereolithography is based on the use of photopolymers, polymers that change material properties when exposed to light, primarily in the ultraviolet range [12]. Exposing it to light results in cross-linking causing the material to harden. Stereolithography can produce products with a wide variety of properties, for example stiffness, thermal resistance, flexibility etc. however the photopolymer can become brittle with extended exposure to light over time.

Advantages

- Good for high resolution parts.
- Average build speed.
- Surface finish is good.
- Little waste, because the liquid which is not exposed to UV can be reused.

Disadvantage

- Expensive technology, because photopolymers are expensive and the process requires that the total barrel is filled.
- Supports need to be designed with CAD or will be automatically designed with SLA software.
- Requires cleaning and curing.
- The liquid photopolymer is toxic and has a pungent smell.
- The photopolymer can become brittle over time, accelerated by extended exposure to light

2.3.2 Digital light processing

With digital light processing a projector is used to expose material with ultra violet light. One can compare it with the beamers used in office presentations. The digital micromirror device (DMD) is the core component of the DLP printer. It starts with a light source. The light source is directed towards the DMD which reflects a digitally controlled light pattern of each cross section of the object through a focussing lens and into a photopolymer resin. The UV light causes the resin to harden and to form the first layer of the object. The recently created layer is then moved upwards. The newly created space between the print and the vat is filled again with fresh photopolymer and the cycle starts over again. With this process the movement of parts is minimised and the entire cross section can be printed in one illumination step, which is faster than drawing the cross section with a laser.

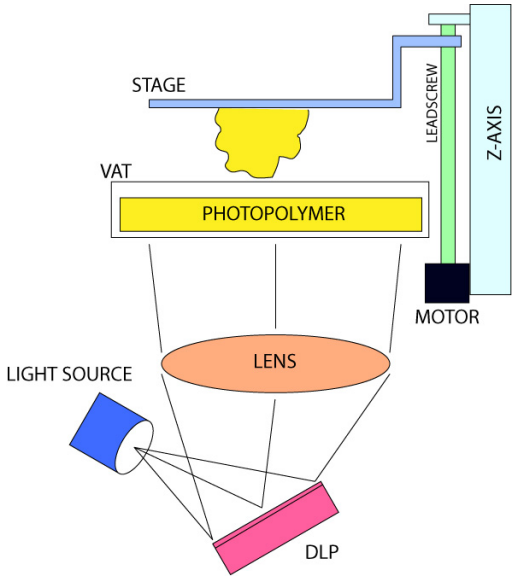

Figure 4: Principle of DLP [5]

Resolution	
Layer thickness	25-150μm
Tolerances	>100μm
Surface roughness	2μm Ra
Supporting material	No
Channels possible	Yes

Table 4: Properties of Digital light processing [6].

Materials used

Just like in stereolithography a photopolymer is used. Photopolymers can have widely varying properties, for example stiffness, thermal resistance, flexibility etc. However the photopolymers can become brittle with increased exposure to light over time.

Advantages

- High resolution, achieved by small layer thickness and tolerances. table 4
- Fast build speed, approximately 2 cm per hour with 50 micron layers [10].
- Relatively cheap
- No moving parts only platform.

Disadvantages

- Requires curing and cleaning of the printed structure.
- The liquid photopolymer is toxic and has a pungent smell.
- The photopolymer can become brittle over time, accelerated by light
- Supports have to be designed with CAD in order to support the material.

2.4 Powder bed fusion

2.4.1 Selective laser sintering

At the University of Texas Carl Deckard and colleagues developed selective laser sintering. The technology was patented in 1989. It uses a moving laser beam and a powder. The laser beam hits the powder causing it to sinter locally. Sintering is a technology where the powder gets heated but doesn't melt. This sintering causes the powder to attach to each other and to form a strong structure. The laser will draw the cross section of the object to form a first layer. The part is build on a platform, after a cross section is finished the platform will lower and a roller adds new powder on top and the process starts again. The excess powder which is not sintered in each layer acts as a support to the part. Therefore no additional material is needed to support the structure during building. Once the printing is completed the object is left to cool and the leftover material can be recovered and recycled. Also with this technology there exists anisotropy in the material due to the additive layer method. The strength of the body is the weakest in the vertical build section. Holes or channels are possible only if you can access them from the outside. When the product is finished there could be stress locations especially when using metals, therefore stress annealing and relieving may be required. Shrinkage occurs most in the Z direction and a small amount in the X and Y direction [22]. The shrinkage arises in the building

process and also in the annealing process. The SLS software will compensate for shrink to ensure right dimensions.

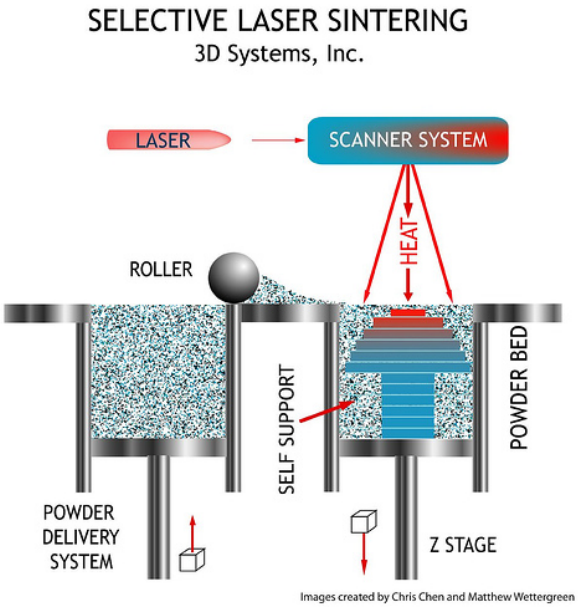

Figure 5: Principle of Selective laser sintering [17].

Resolution	
Layer thickness	75-150μm
Tolerances	>50μm
Surface roughness	7-10μm Ra
Supporting material	No, but excess powder supports
Channels possible	Yes, but hard to remove powder from channel

Table 5: Properties of Selective laser sintering [24].

Materials used

If a material is in powder form and it is possible to be sintered, it should work in this system. Therefore SLS can produce objects from a wide range of available powder materials. Thermoplastics such as Nylon, Polystyrene and Polyamide can be used. Also metal powders including steel, alloy mixtures, titanium and composites are used and even ceramic powders are used.

Advantages

- No supports needed, excess powder supports
- Wide range of materials can be used.
- Build speed is medium to fast.
- High strength parts, greater than 99 percent density can be achieved.
- The cost of the powdered material is low to moderate.
- Left over material can be reused.

Disadvantages

- Technology is expensive: High equipment cost, high energy requirements due to laser.
- Low resolution compared to other technologies.
- Stress locations can occur especially in metals.

2.5 Sheet lamination

2.5.1 Laminated object manufacturing

The technology was developed by Helisys of Torrance. The first device was sold in 1991. It's a different kind of 3D print solution. It starts with a feed mechanism. A roll of adhesive-coated paper, plastic or metal is unrolled and a layer of material is placed over the platform. A heated roller applies pressure to bond the new layer to the layer below. With this process the layers are successively glued together. A laser cuts the outline of the object, after the cut is completed the platform lowers and a new sheet of material is advanced on top of the previously deposited layers. The extra material remains in place for supporting the object, therefore the laser has to cut a square with approximately the same size as the platform to cut the support material from the roller. This causes a post processing step, because the supporting material needs to be removed. Objects printed with this technique can additionally be modified by machining or drilling after printing [9]. The dimensional accuracy is slightly less compared to selective laser sintering and stereolithography. The tensile strength of the finished object is highly anisotropic, with the weakest strength in the vertical direction. Also the object hardly shrinks during fabrication.

Materials used

The materials used in LOM are often plastics, metals and paper. The paper models have wood like characteristics.

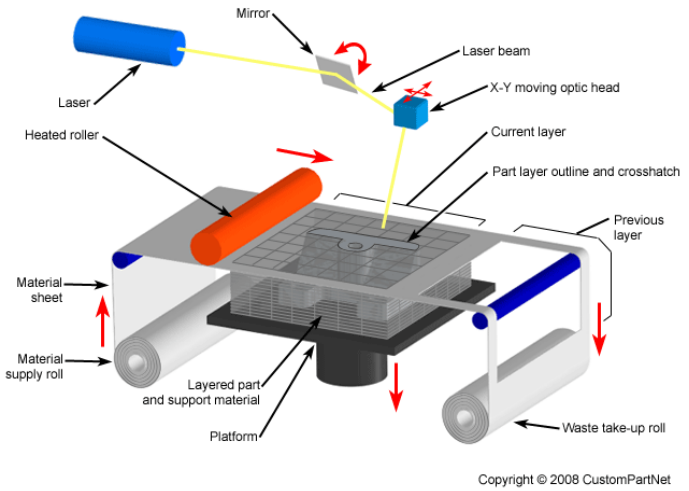

Figure 6: Principle of LOM [15].

Resolution	
Layer thickness	50-200μm
Tolerances	>100μm
Surface roughness	30-40μm Ra
Supporting material	Yes, excess material supports
Channels possible	Yes, but hard to remove excess material from channel

Table 6: Properties of LOM [24].

Advantages

- Building speed is medium to fast.
- No chemical reaction is required.
- Low cost due to available raw materials.
- No supports needed, because excess material supports.

Disadvantages

- Dimensional accuracy is slightly less.
- Additional machining or drilling is necessary.
- A lot of waste material.
- Cannot create hollow parts.

- Highly anisotropic.
- Surface finish is poor compared to other additive processes.

2.6 Material Jetting

2.6.1 Objet Printing

The Objet printing is a 3D building process which combines the techniques of Stereolithography and Inkjet Printing. The method of building a layer is the same as an inkjet printer used to print documents. It uses an array of inkjet print heads to drop small drops of material and supporting material on the platform to form the layer. After each layer is deposited the layer is cured by an UV lamp. Therefore no more separate curing processes are needed. This process is continued till the object is finished. The most common application of objet printing is prototypes which are used for form and fit testing. There exist two types of supporting material: a photopolymer which can be washed away with pressurized water and a wax support material which can be melted away. Also with this technology their exist anisotropy in the material due to the additive layer method [21]. Holes or channels are possible only if you can reach them from the outside. The shrinkage of Objet printing is closely the same as stereolithography.

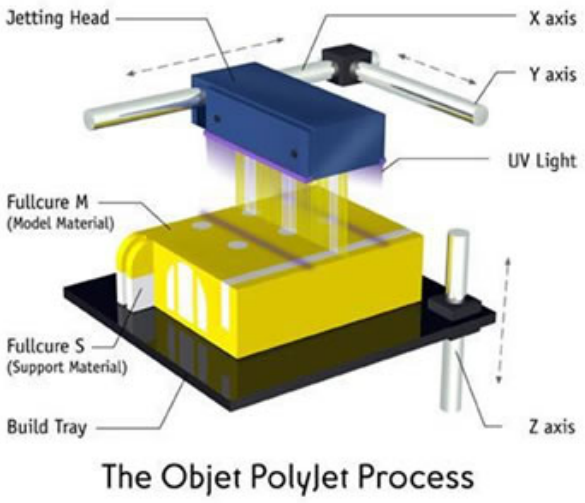

Figure 7: Principle of Objet Printing [16].

Resolution	
Layer thickness	15-100μm
Tolerances	>20μm
Surface roughness	Excellent
Supporting material	Yes
Channels possible	Yes

Table 7: Properties of Objet printing [11].

Materials used

Just like in stereolithography this technology uses photopolymers. Photopolymers have a wide variety of properties, for example stiffness, thermal resistance, flexibility etc. however the photopolymer can become brittle with increased exposure to light over time.

Advantages

- Very good accuracy.
- No separate curing process is needed.
- Build speed is medium to fast.

Disadvantage

- The photopolymer can become brittle over time.
- Requires cleaning because supporting is used.

2.7 Binder Jetting

2.7.1 Binder Jetting

Binder jetting was developed by Ely Sachs and Mike Cima at the Massachusetts Institute of technology in 1993 [3]. This additive manufacturing method works by spraying a liquid binder onto a bed of powder. The printing starts with moving up the powder supply bin and spreading the first layer of powder on the build platform by the levelling roller (figure 8). The inkjet printer head applies a liquid bonding agent to solidify the powder into a cross-section. After each cross section is finished, the build platform will be lowered, the powder supply bin lifted and the levelling roller will deposit a new layer of powder on the platform to form the next layer. This process is repeated until the object is finished. The loose powder surrounds and supports the object in the build chamber. When the object is finished the loose powder can be reused and any excess powder on the body can be blown off by pressurized air. The distinction between other additive technologies is that binder jetting has the ability to print

Resolution	
Layer thickness	90μm
Tolerances	>130μm
Surface roughness	Good
Supporting material	No, but excess powder supports
Channels possible	Yes

Table 8: Properties of Binder Jetting [2].

in colour. The parts produced with this technology are basically particles glued together. This will result in fragile parts with limited mechanical properties. The shrinkage of this process is small, because only glue is needed to attach the powder to each other.

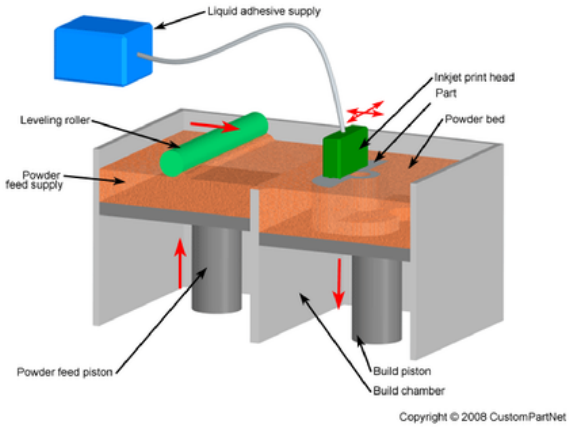

Figure 8: Principle of Binder Jetting [13].

Materials used

There is a wide range of materials which can be used for this additive process. Composites, metals, glass, plastics and sand are used. The combination for pairing binder agents to powder material creates a wide range of material properties.

Advantages

- Less expensive technology.
- Rather fast build speed.
- Ability to print in colors.

- Wide range of material which can be used.

Disadvantages

- Limited mechanical properties, because the binder solidifies using a liquid bonding agent. This will result in low Tensile Strength and Young's Modulus.

2.8 Conclusion of techniques discussed

The commercially available 3D printing processes were treated in the previous sections. Table 9 gives a comparison of the technologies discussed with respect to cost, resolution, mechanical characteristics, material range and build speed. The Fused Deposition Modeling technology is the most suitable technology for printing 3D objects for consumer use, because it is suitable for desktop use, low cost with sufficient resolution and good mechanical characteristics. Only the build speed is relative slow. Objet printing or Digital light processing are the most suitable technologies for research, because very small parts can be produced with very good resolution.

Technologies	Cost	Resolution	Mechanical	Material range	Build speed
FDM	++	-	+	+	–
SLA	–	++	-	+	+
DLP	+	++	-	+	++
SLS	–	+	++	++	+
LOM	++	–	–	-	+
OP	-	++	-	+	+
BJ	++	+	–	++	+

Table 9: Comparison of additive manufacturing systems.

3 Test structure designs

3.1 Investigation

First the objects will be investigated with respect to shape. The properties we are interested in are:

- Resolution, what is the minimum size of a channel or block?
- Dimensional accuracy, what is the difference between the real model and the digital model?
- Surface roughness

These properties will give an indication of the usability and will give further understanding of the printing process. The investigations will focus on finding the mechanical properties of 3D printed structures with the aim to print as small as possible. To achieve this the most accurate available print technologies will be used. The Digital light processing and the Objet printing will be used, because of the small layer thickness and good accuracy.

Because of the assumed anisotropy in the 3D printed technology the mechanical properties have to be investigated in all directions. The properties of interest are:

- The Young's modulus: E
- The Shear Modulus: G

There are several methods available to experimentally measure the Young's Modulus of objects of millimeter size. To measure the Shear Modulus is a different story, therefore some creative solutions are necessary.

In order to investigate the mechanical properties of 3D printed small objects, structures need to be designed. The test structures will be designed with the program SolidWorks. SolidWorks is solid modelling CAD (computer-aided design) software that runs on Microsoft Windows and is produced by Dassault Systems SolidWorks Corp [19].

3.2 Orientations

In order to be consistent and systematic in the investigation a Cartesian coordinate system is chosen. Figure 9a represents the coordinate system. The structures or gaps will be designed on those planes. Figure 9b represents the orientations of the printed layers. These orientations will be used in all designs.

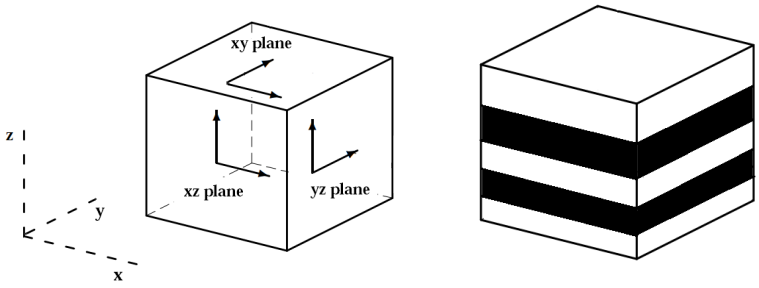

(a) xyz planes (b) Orientations layers

Figure 9: Cartesian coordinate system

3.3 Minimal block and channel thickness

A cubic square of 1 cm^3 is used as a base. To investigate the minimal block and channel thickness, block and hole triangles are used. The triangles are designed with one sharp angle in order to estimate the minimum size. The dimensions of the triangles are shown in table 10.

Dimensions of the triangle	
Lenght	7.3 mm
Height	2 mm
Width	3.25 mm
Top angle	25 Degrees

Table 10: Dimensions of the designed triangle

3.3.1 Solidworks design

The triangular blocks and holes are orientated in all six possible orientations figure 9a. Figure 10 represent the solid works design. Six triangular blocks and six triangular holes are designed in order to measure the minimum block and channel thickness in all six orientations.

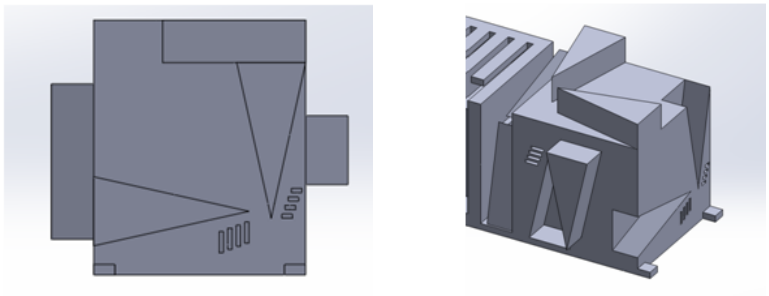

(a) Top view (b) 3D view

Figure 10: Orientation of blocks

3.3.2 Measurement procedure

A microscope from the Transducers Science and Technology group is used to investigate the triangular blocks and holes. A CCD camera is mounted on the microscope to capture the images. The CDD camera is equipped with a measuring system to estimate the minimum block and hole size. An electron microscope is used to investigate the surface of the blocks.

3.4 Dimensional accuarcy

It is essential to know the dimensional accuracy of printed objects to investigate the usability of 3D printing technologies. An inline method is used to measure the deviation of printed blocks and holes. A combination of 3 blocks or holes are placed in a certain pattern. The middle block is placed a known distance lower than the other two blocks figure 11a. If the blocks shrink due to deviations the 3 blocks should line up figure 11b. This will give an indication how large the deviation is. A multiple pair of blocks and holes with different separation distances will be designed.

(a) three blocks aligned for inline measurements (b) Inline

Figure 11: Orientation of blocks

3.4.1 Solidworks design

In order to investigate the deviation of the blocks, two sizes of square blocks and holes are used. The dimensions of the blocks are 1 mm and 0.6 mm in length width and height. The blocks and holes will be placed in al six orientations figure 9a. The SolidWorks design represents the test structure. A cubic square of 1 cm^3 is used as a base.

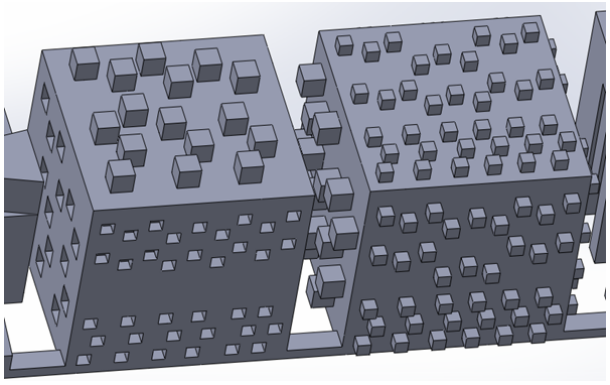

Figure 12: Solid works design

3.4.2 Orientations of the blocks

The blocks and holes are placed with a known seperation distance. Figure 13 represents the orientation of the blocks and holes. Those structures and holes will be placed on the xy yz and xz-planes, this will result in 12 planes of blocks and holes. The separation distances of the blocks and holes are tabulated in table 11.

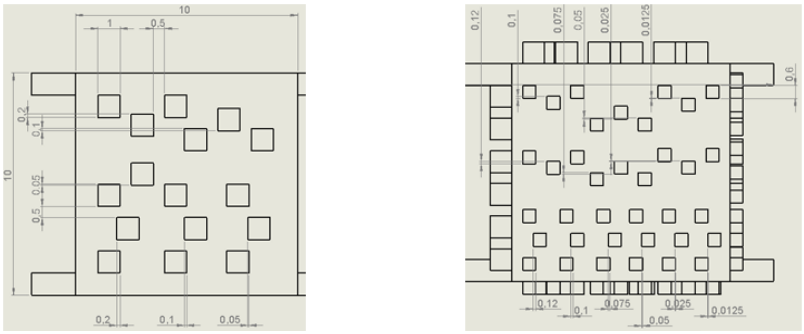

(a) 1mm blocks (b) 0.6mm blocks

Figure 13: Orientation of blocks and holes.

Seperation distances						
1 mm blocks	200 μm	100 μm	50 μm			
0.6 mm blocks	120 μm	100 μm	75 μm	50 μm	25 μm	12.5 μm

Table 11: Separation distances of the blocks.

3.4.3 Measurement procedure

With the use of a microscope the distance at which the blocks will line up are investigated. A CCD camera is connected to the microscope to capture the images. This results will give an estimation of the deviation of printed blocks or holes.

3.5 Dynamic design cantilever

A dynamic approach is used to investigate the Young's modulus of the printed structures. A cantilever, a beam which is fixed at only one end, is used in the dynamic measurements. It is a very suitable object to use for the measurements, since it can be easily brought into resonance, where the resonance frequency depends on the mass and beam stiffness. It is assumed that the cantilever only deforms in the linear elastic region. Then with the Euler-Bernoulli beam theory the frequency of the i^{th} mode be predicted. The first resonance frequency of a cantilever is given by equation 1.

$$f(0) = \frac{(1.875)^2 h}{2\pi l^2}\sqrt{\frac{E}{12\rho}} \tag{1}$$

Where L is the length, ρ is the mass-density, h is the thickness and E is the Young Modulus of the cantilever. With the resonance frequency measured in the test, dimensions carefully checked by microscope and the mass density measured by Archimedes principle (the volume with a graduated cylinder and mass with a weighing unit) , we can calculate the Young's Modulus of the cantilever. Figure 14 represents the sketch of a solid structure with cantilever.

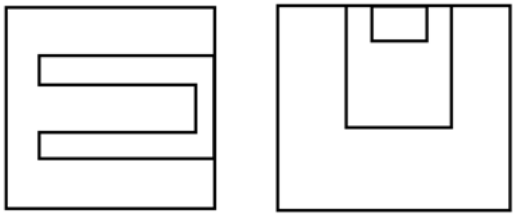

Figure 14: Sketch of cantilever

3.5.1 Solidworks design dynamic cantilever

The resonance frequency of the cantilever will be measured. Therefore the test structure should be designed in a way such that it is measurable with the available equipment at the TST chair: the gap between the cantilever and rigid part should be small in order to enable the use of a reference beam in the measurement of the resonance frequency, the open space below the cantilever should be large to minimise air resistance figure 15c. The design for the Objet printer figure 15a has free designed cantilevers. The Objet technology makes use of supporting material to support overhanging structures. Figure 15b, represents the design of the DLP printer. The cantilevers are supported by printed material to prevent deflection during printing, because the DLP technology has no support material. Those supports have to be removed manually before the cantilever can be tested.

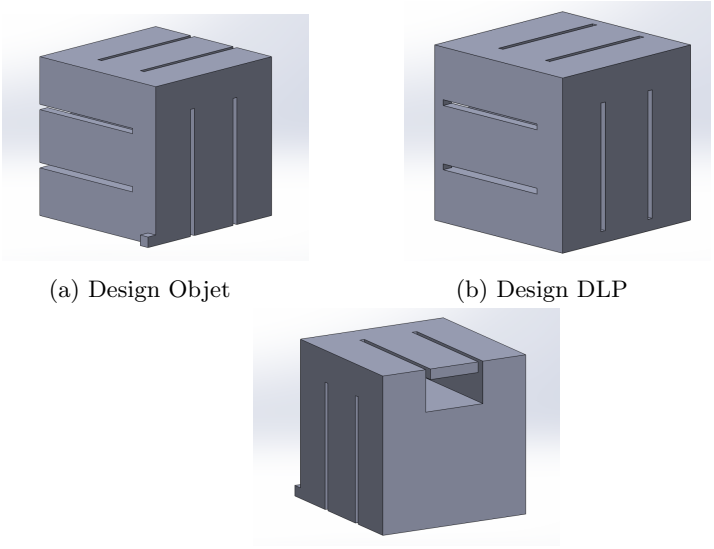

(a) Design Objet

(b) Design DLP

(c) Open space below cantilever

Figure 15: Orientation of cantilevers.

3.5.2 Measurement procedure

The resonance frequency should be measured to calculate the Young's Modulus of the cantilevers. A speaker is used to excite the cantilever from 500Hz till 10000Hz. The displacement of the cantilever will be max at the resonance frequency. A laser-vibrometer is used to measure the displacement of the cantilever in order to measure the resonance frequency. The first laser-spot is placed at the cantilever and the second at the rigid part. In order to measure the real displacement the software will subtract the phase differences of the the two beams.

Figure 16 represents the position of the lasers on the test structure. The light absorption of the printed structures is large, therefore a very small part metal layer is deposited on the tip of the structure to increase reflection.

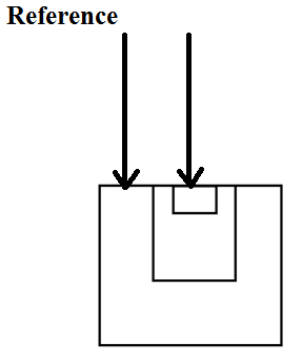

Figure 16: Position Lasers

3.5.3 Error analysis

An error analysis is done in order to estimate the error made during testing. Equation 2 describes the standard deviation of the Young's Modulus calculated. This error is of crucial importance in order to draw conclusions. Errors can be made by measuring the resonance frequency $F_{\max}$, the height h, the length L and the Density ρ of the cantilever.

$$\frac{\Delta E}{E} = \sqrt{\left(2\frac{\Delta F_{\max}}{F_{\max}}\right)^2 + \left(2\frac{\Delta h}{h}\right)^2 + \left(4\frac{\Delta L}{L}\right)^2 + \left(\frac{\Delta \rho}{\rho}\right)^2} \tag{2}$$

3.6 Static design cantilever

There are lots of techniques to determine the Young's modulus of material statically. A tensile test can be executed for example, but for small printed objects it will be difficult, because the displacements are small and the forces are relative high. To apply large forces a very stiff measurement setup is needed , therefore it is not very suitable for our purpose and a better solution is a cantilever deflection measurement. A cantilever is already used for the dynamical model. The cantilever is a very suitable structure to deflect and with the static measurement the mass has no effect, thereby excluding one potential unknown parameter. To deflect the cantilever a force is applied at pre-specified positions on the cantilever. The amount of force needed to displace a cantilever is much smaller compared to a tensile test, furthermore the displacement is much larger. This makes it more suitable to measure the Young's Modulus statically. Equation 3 represents the deflection of a cantilever beam when a force is applied at

length l from its fixed side and where the deflection is measured at that same distance l.

$$\Delta x = \frac{Pl^3}{3EI} \tag{3}$$

Δx is the end displacement, l is the length, E is the Young's modulus, P is the force applied at the end and I is the inertia of the cantilever beam. This equation will be used to determine the Young's modulus of the structure. The equation can be verified by measuring at different positions of the cantilever. Six small points will be designed at different lengths.

3.6.1 Solidworks design static cantilever

There is a block of 1 cubic centimeter used as a base platform which will be connected to a weighing unit (scale). Three cantilevers in the x, y and z directions are mounted on the base platform. Six small holes on each cantilever are designed. To displace the cantilever a force is applied at one of the holes. The Young's modulus can be determined with this design, but it is also possible to verify if the stiffness also decreases with length to the third power according to theory (3). The cantilever design will be printed with both Objet and DLP printers. Figure 17a and Figure 17b represents the Objet design and DLP design respectively. For the DLP design again some supports, which should be removed after printing, are included. The dimensions of the cantilevers are tabulated in table 12.

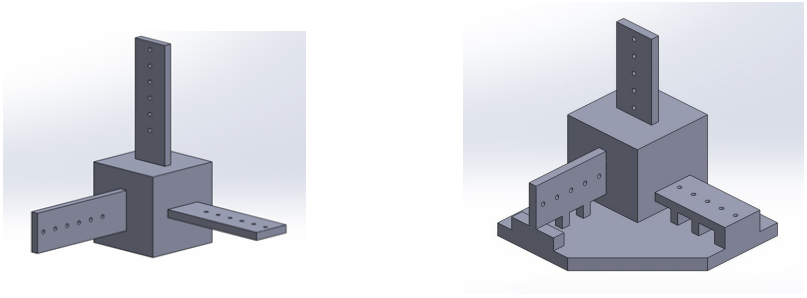

(a) Objet design (b) DLP design

Figure 17: Cantilever structures

Dimensions of cantilever	
Lenght	15 mm
Width	5 mm
Height	1 mm
Distance between holes	2 mm

Table 12: Dimensions of cantilevers

The holes designed in the cantilever will influence the behaviour, because they will reduce the thickness of the cross-section of the beam, this reduction will lead to a larger displacement according to equation 3. Therefore a finite element simulation was executed to measure the increase in displacement due to the holes in the cantilever. The cantilever will displace 0.6 percent more due to the holes. This was regarded as a very small error which can be neglected relative to other errors and no further actions to counteract the effects were undertaken.

3.6.2 Measurement procedure

The rigid block is mounted on a weighing unit. A displacement is applied with a needle mounted on a translation table, this displacement can be read-out with micrometer accuracy. Figure 18 represents the testing method. The testing equipment is not totally rigid, but has a certain stiffness. Therefore a compensation has to be made for the stiffness of the testing equipment. Equation 4 represents the total stiffness K_{eq}, The cantilever stiffness K_{c} and the equipment stiffness K_{op}.

$$\frac{1}{K_{\text{eq}}} = \frac{1}{K_{\text{c}}} + \frac{1}{K_{\text{op}}} \tag{4}$$

First the equipment stiffness is measured to compensate for the K_{op}. It is crucial with the statical measurement that the measurement time will be short, because otherwise creep will influence the displacement. The max displacement of the tip should not exceed 1mm in order to stay in the elastic region.

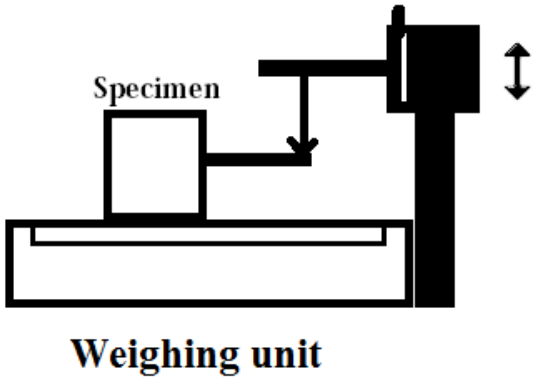

Figure 18: Measurement setup

3.6.3 Error analysis

Equation 5 describes the error of the calculated Young's Modulus using standard deviation. Errors can be made by measuring the spring constants, K_{op} and K_{eq}, the lenght L, the width b and height h of the cantilever. All those quantities will influence the measurement accuracy. Therefore it is crucial to measure as precise as possible especially the length L and height h, because they increase to the third power .

$$\frac{\Delta E}{E} = \sqrt{\left(\frac{\Delta K_{\mathrm{c}}}{K_{\mathrm{c}}}\right)^2 + \left(3\frac{\Delta L}{L}\right)^2 + \left(\frac{\Delta I}{I}\right)^2} \tag{5}$$

$$\frac{\Delta I}{I} = \sqrt{\left(\frac{\Delta b}{b}\right)^2 + \left(3\frac{\Delta h}{h}\right)^2} \tag{6}$$

$$\Delta K_{\mathrm{c}} = \sqrt{(\Delta K_{\mathrm{op}})^2 + (\Delta K_{\mathrm{eq}})^2} \tag{7}$$

3.7 Shear modulus measurement

A second interesting mechanical property is the shear modulus, also called modulus of rigidity, and denoted by G. The shear modulus is defined as the ratio of shear stress to shear strain. Equation 8 represents the definition of the shear modulus. Where τ is the shear stress and γ the shear strain, A the area on which the force acts, Δx the transverse displacement, F the force and l the initial length. Figure 19 represents the deformed shape of a cube when a shear force is applied.

$$G = \frac{\tau}{\gamma} = \frac{Fl}{A\Delta x} \tag{8}$$

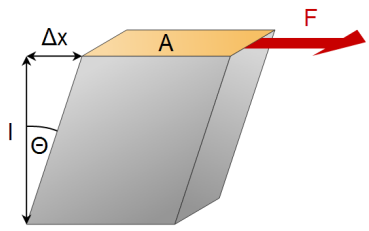

Figure 19: Shear modulus principle [18].

3.7.1 Solidworks design

A test structure is designed with Solid Works to measure the shear modulus. Figure 20 represents the design. A cube with sides of 5 mm is placed between

two blocks. On this cube a shear force will be applied. Table 13 represents the dimensions of the structure. A hole is made at the place where the force will be applied. A finite element simulation was executed to estimate the position of the hole to maintain only vertical movements of the upper block. The blocks will be printed in all six orientations.

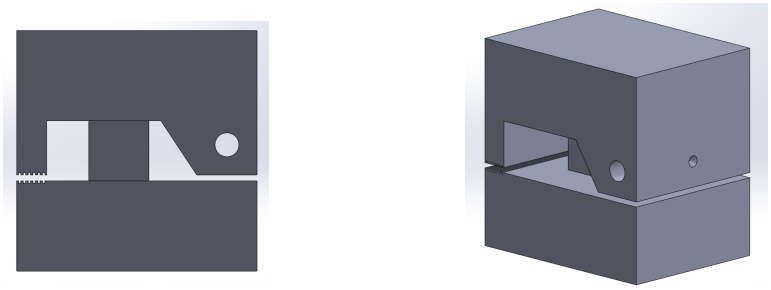

(a) Side view (b) Shear design 3D

Figure 20: Cantilever structures

Dimensions of G design	
Lenght	20 mm
Width	15 mm
Height	20 mm

Table 13: Dimensions of G design.

3.7.2 Measurement procedure

The bottom of the structure will be fixed and a force will be applied in the positive X direction on the upper block, this will be done with a chord with masses at the end, causing the cube to shear. A displacement sensor will be placed at the left side of the upper block in order to measure the displacement figure 21. The displacement should not exceed 100 micrometer in order to stay in the elastic region.

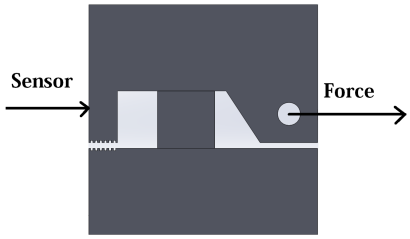

Figure 21: Measurement procedure

3.7.3 Error analysis measurement shear modulus G

The square block could also have an extra displacement due to bending, described by the Euler-Bernoulli beam theory. Experimental measurements show that these equation is only valid for long, slender beams made of isotropic materials with solid cross-sections [23]. The test structure is a square block, therefore the influence of bending of the block will be neglected and only shear will be assumed.

To estimate the accuracy of the results an error analysis is done. Again the standard deviation is used. Equation 9 describes the standard deviation of the Shear Modulus. Errors can be made by measuring the force F, the length L, the area A and the displacement x.

$$\frac{\Delta G}{G} = \sqrt{\left(\frac{\Delta F}{F}\right)^2 + \left(\frac{\Delta L}{L}\right)^2 + \left(\frac{\Delta A}{A}\right)^2 + \left(\frac{\Delta x}{x}\right)^2} \tag{9}$$

4 Dimensional Results

4.1 The layer thickness and pixel size of DLP.

Before printing the real test structures the hoses and the print bin were cleaned intensively to improve accuracy. The cleaning of the bin induced a major improvement of the accuracy of the structures, because the UV light scattering and deflection by the dirt in the bin were largely reduced.

An optical microscope was used to investigate the layer thickness. To investigate the pixel size an electron microscope was used. It was not possible to measure the layer thickness of the Objet structures because of the rough surface area. The layer thickness and pixel size are tabulated in table 14.

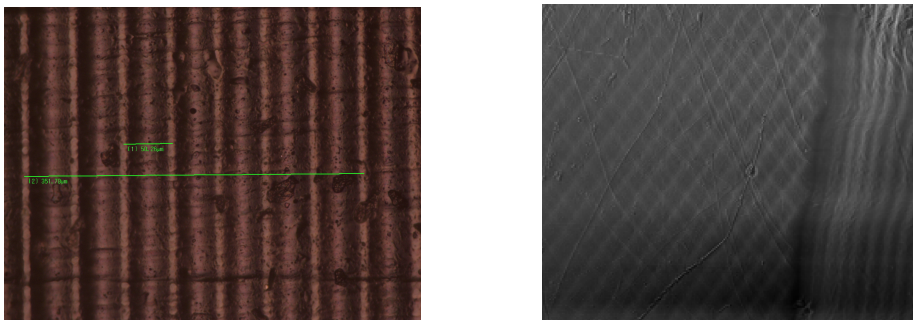

(a) Layer thickness (b) Pixels

Figure 22: DLP results

Layer thickness	± 50 μm
Pixel size	50 μm

Table 14: DLP specifications

4.2 Squareblocks and Squareholes

The block pairs were analyzed with a microscope. A CCD camera was used to capture the images. The coordinate system and the layer orientation are shown again in figure 23 to clarify which plane is analysed. The light absorption of the printed structures is large, therefore some pictures are relative dark in the presented results.

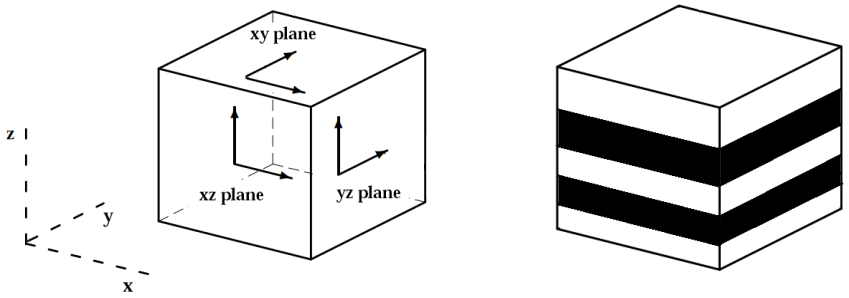

(a) xyz coordinate system (b) Layer orientation

Figure 23: Cartesian coordinate system

4.2.1 Blocks of 1 mm

Measurement in xy-plane DLP and Objet.

The blocks on the xy-plane printed with the DLP and Objet were investigated. Figure 24a, b and c present the blocks printed with the DLP and figure 24d, e and f present the blocks printed with the Objet. It is clear that the resolution of the DLP in the xy-plane is better.

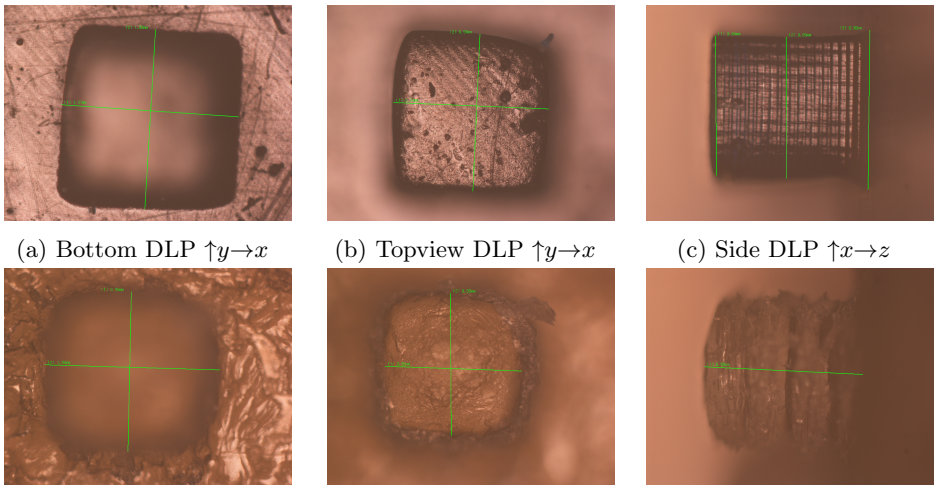

(a) Bottom DLP $\uparrow y \rightarrow x$ (b) Topview DLP $\uparrow y \rightarrow x$ (c) Side DLP $\uparrow x \rightarrow z$

(d) Bottom Objet $\uparrow y \rightarrow x$ (e) Topview Objet $\uparrow$y$\rightarrow x$ (f) Side Objet $\uparrow x \rightarrow z$

Figure 24: Pictures of xy-plane

The results of the inline method of the blocks in pairs are tabulated in table 15. Microscope observations showed that the 3 blocks where at the same line at approximately 50 μm for the DLP and 100 μm for the Objet in both directions.

This observation indicates that the printed blocks are smaller compared to the designed blocks in CAD.

Accuracy	DLP	Objet
x-direction	≈50 μm	≈100 μm
y-direction	≈50 μm	≈100 μm

Table 15: Accuracy achieved by DLP and Objet printer in the xy-plane.

Measurement in the xz-plane

The same procedure is used for the xz-plane.

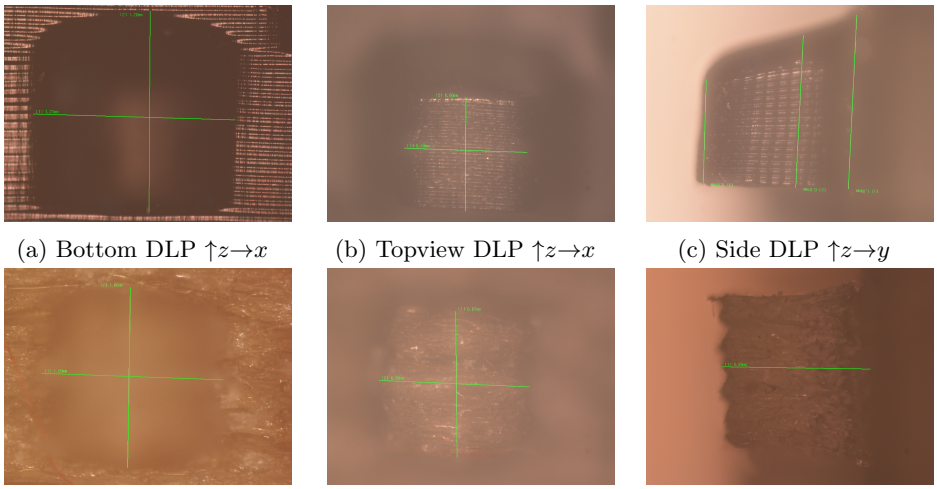

(a) Bottom DLP $\uparrow z \rightarrow x$ (b) Topview DLP $\uparrow z \rightarrow x$ (c) Side DLP $\uparrow z \rightarrow y$

(d) Bottom Objet $\uparrow z \rightarrow x$ (e) Top view Objet $\uparrow z \rightarrow x$ (f) Side Objet $\uparrow z \rightarrow y$

Figure 25: Pictures of xz-plane.

Accuracy	DLP	Objet
z-direction	≈200 μm	≈100 μm
x-direction	≈200 μm	≈100 μm

Table 16: Accuracy achieved by DLP and Objet printers in xz-plane

Figure 25c indicates a limitation of the Digital Light Printer. It is hard to construct a horizontal beam, because the first layer of the beam is 50 μm thick and when the platform moves up to print the next layer, the first layer bends downwards (due to gravity and surface tension). Beyond approximately 500 μm thickness the layers are straight. Table 16 indicates that the Objet will reach

better accuracy in the xz-plane compared to the DLP. Again the printed blocks are smaller compared to the designed blocks in CAD.

Measurement in the yz-plane

The same procedure is used for the yz-plane.

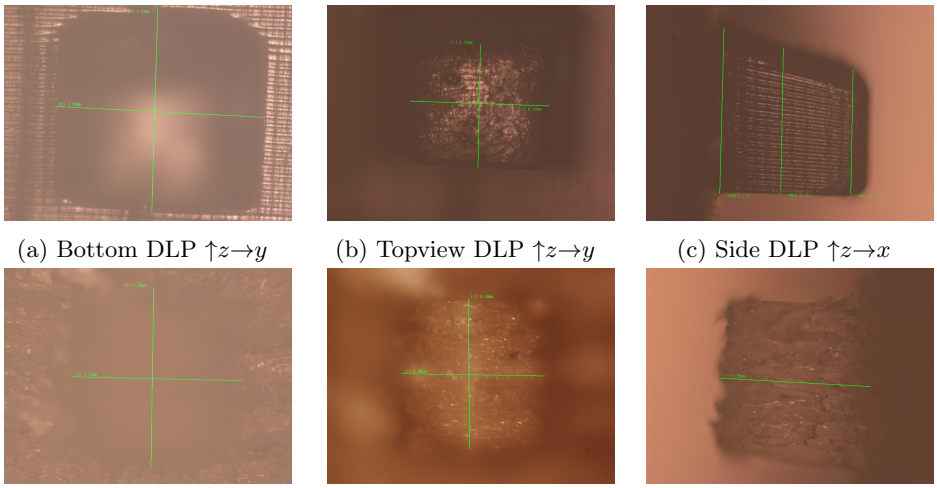

(a) Bottom DLP $\uparrow z \rightarrow y$ (b) Topview DLP $\uparrow z \rightarrow y$ (c) Side DLP $\uparrow z \rightarrow x$

(d) Bottom Objet $\uparrow z \rightarrow y$ (e) Topview Objet $\uparrow z \rightarrow y$ (f) Side Objet $\uparrow z \rightarrow x$

Figure 26: Pictures of structures in the xz-plane

Accuracy	DLP	Objet
z-direction	$\approx$200 μm	$\approx$100 μm
x-direction	$\approx$200 μm	$\approx$100 μm

Table 17: Accuracy achieved by the DLP and Objet printers in the xz-plane

The same thing is happening in the yz-plane with the DLP figure 26c shows the overhanging beam. And again the Objet has due to the supporting material a better accuracy in the yz-plane compared to DLP.

4.2.2 Blocks of 0.6 mm

It was not possible to remove the supporting material without damaging the 0.6 mm blocks and holes of the Objet, therefore no conclusion can be drawn for the Objet blocks, and no comparison can be made between DLP and Objet. However the blocks of the DLP can still be analysed. The deviation distances are tabulated in the table 18. This also confirms that the xy-plane has the best

resolution. The pictures shown are from the xy-plane. Figure 27c represents the side view of the block.

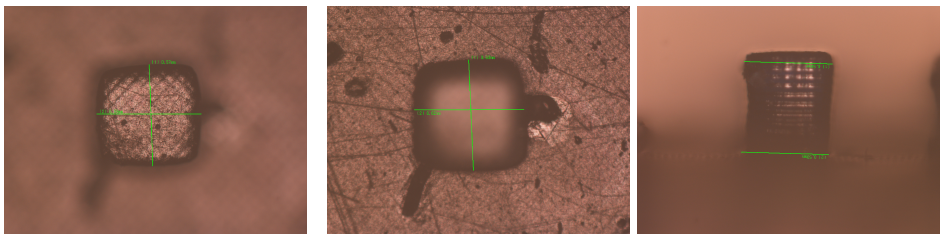

(a) Top view $\uparrow y \rightarrow x$ (b) Bottom view $\uparrow y \rightarrow x$ (c) Side view $\uparrow y \rightarrow z$

Accuracy	xy plane	xz plane	yz plane
y direction	25μm		$\approx$120μm
x direction	25μm	$\approx$120μm	
z direction		$\approx$120μm	$\approx$120μm

Table 18: Accuracy of blocks of 0.6mm

4.2.3 Holes of 1 mm printed by DLP and Objet

Microscope observations showed that the deviation of the holes where slightly bigger compared to the blocks. It was hard to remove the support material without damaging the holes of the Objet structures, this will limited the design freedom.

Due to the fact that there is no support material in the DLP technology the holes in the xz and yz-plane have a larger deviation. Table 19 indicates the accuracy of the DLP holes and table 20 indicates the accuracy of the Objet holes. Again is seen that the Objet reach beter accuracy in all directions, because of the supporting material.

Accuracy of DLP holes	xy-plane	xz-plane	yz-plane
y-direction	Unknown		$\approx$200 μm
x-direction	Unknown	$\approx$200 μm	
z-direction		$\approx$200 μm	$\approx$200 μm

Table 19: Accuracy of 1 mm holes printed with DLP.

Accuracy of Objet holes	xy-plane	xz-plane	yz-plane
y-direction	100 μm		$\approx$150 μm
x-direction	100 μm	$\approx$150 μm	
z-direction		$\approx$150 μm	$\approx$150 μm

Table 20: Accuracy of 1 mm holes printed with Objet.

4.3 Minimum block size

Mesurement in xy-plane

The Triangles in the xy-plane of the DLP and Objet structures were analysed. Figure 28 presents the triangles for DLP and Objet. The miminum block size is tabulated in table 21. Microscope observations showed that the DLP printer was able to print smaller blocks in the xy-plane.

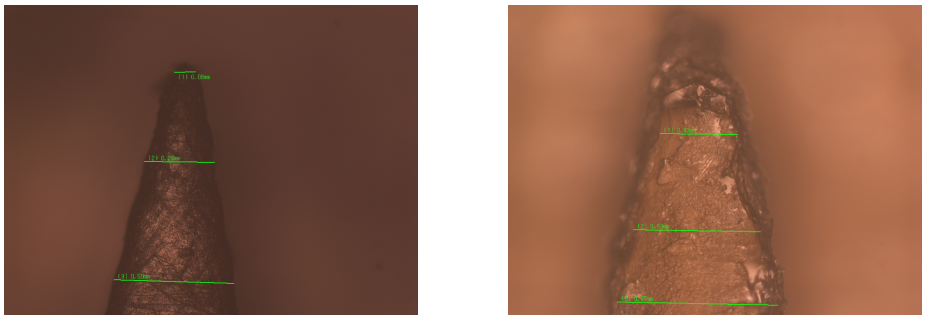

(a) DLP triangle y-direction

(b) Objet triangle y-direction

Figure 28: Pictures of xy-plane.

Min block size	DLP	Objet
y-direction	150 μm	300 μm
x-direction	150 μm	300 μm

Table 21: The minimal block size in xy-plane

Measurement in xz-plane

The Triangles in the xz-plane of the DLP and Objet structures were analysed. It was seen that the Objet structures show te same resolution as in the xy-plane, the supporting material supports the triangle sufficient to ensure right dimensions. The DLP Triangles are also deflected due to the absence of supports of the overhanging parts, which will increase the minimum block size. Table 22

presents the minimal block sizes of DLP and Objet printed triangles in the xz-plane.

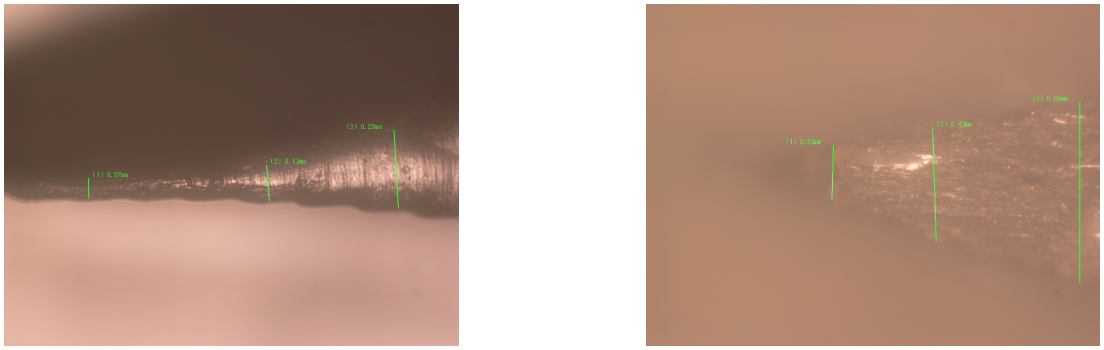

(a) DLP x-direction

(b) Objet x-direction

Figure 29: Pictures of xz-plane

Min block size	DLP	Objet
x-direction	500 μm	300 μm
z-direction	500 μm	300 μm

Table 22: The minimal block size in xz-plane

Measurement in yz-plane

The Triangles in the xz-plane of the DLP and Objet structures were analysed. Table 23 represents the minimum block size of DLP and Objet structures.

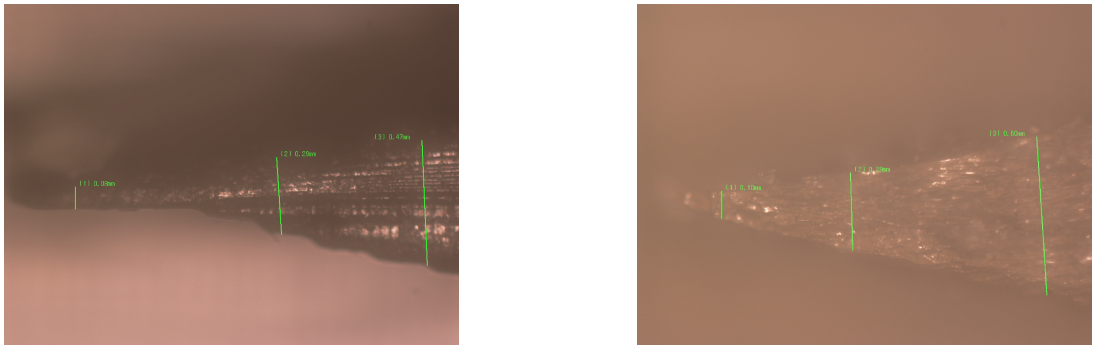

(a) DLP y-direction

(b) Objet y-direction

Figure 30: Pictures of yz-plane

Min block size	DLP	Objet
y-direction	500 μm	250 μm
z-direction	500 μm	300 μm

Table 23: The minimal block size in yz-plane

4.4 Minimum hole size

The triangular holes of the DLP and Objet structures were analysed to investigate the minimum hole sizes. It was seen for the DLP structures that the xy-plane achieved the best resolution. Due to gravity and the absence of support the other planes have larger values. Table 24 presents the minimum hole size of DLP structures. The structures printed with the Objet overall have a better resolution. Table 25 presents the minimum hole size of Objet structures. It has to be kept in mind though, that one should be able to remove the support material manually which can negatively influence the minimum hole size.

Minimum hole size of DLP	xy-plane	xz-plane	yz-plane
y-direction	150 μm		500 μm
x-direction	150 μm	500 μm	
z-direction		500 μm	500 μm

Table 24: Minimum hole size of DLP printed structures.

Minimum hole size of Objet	xy-plane	xz-plane	yz-plane
y-direction	400 μm		400 μm
x-direction	400 μm	400 μm	
z-direction		400 μm	400 μm

Table 25: Minimum hole size of Objet printed structures.

4.5 Conclusion

DLP printed structures: It was seen that the DLP printer was able to print small structures with minimal features of ≈150 μm in the xy-plane. The layer thickness and pixel size are ≈50 μm. The accuracy of the printer is best in the xy-plane and will negatively be influenced by gravity and surface tension in the xz and yz-planes. This effect will limit the technology, because extra structures have to be designed, and cut out afterwards, to support overhanging structures. The surfaces of the DLP structures are very smooth compared to the Objet structures.

Objet printed structures: The Objet was able to print small structures with minimal features of ≈300 μm in all directions. It was not possible to estimate the layer thickness, because the surface-area was too rough. The accuracy is approximately equal in all directions ≈100 μm, in part because supporting material supports overhanging blocks during printing, ensuring right dimensions and shape. However the support material is hard to remove from holes or channels, therefore holes or channels have to be designed larger than ≈1 mm to be able to remove the support material.

5 Young's Modulus results

5.1 Dynamic Young's Modulus results

To calculate the Young's Modulus, the resonance frequency of cantilever beams was measured. Figure 31 indicates the resonance peak of one such cantilevers. A reference measurement was done with both laser-beams pointed at a rigid part of the printed structure. This was done to verify that the peak is really the cantilever resonance peak, and not some noise or vibration from (parts in) the measurement system. Figure 32 indicates the noise of the measurement system where the cantilever resonance peak is clearly absent.

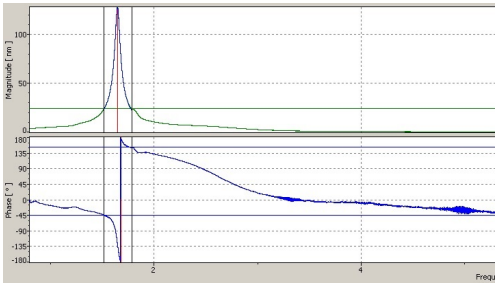

Figure 31: Resonance peak of cantilever

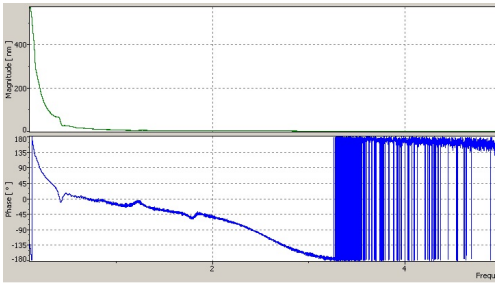

Figure 32: Noise

Table 26 presents the resonance frequencies and the Q-factor as measured for the cantilevers that were printed by Objet. Six possible orientations are measured. $C_{x,y,z}$ indicates the direction of the cantilever, $F_{x,y,z}$ indicates the direction of motion.

	Cantilever direction	Motion direction	Resonance freq	Q
xy-plane	C_x	F_z	1646.1 Hz	33.9
xy-plane	C_y	F_z	1650.8 Hz	35.1
xz-plane	C_x	F_y	1218.8 Hz	17.5
xz-plane	C_z	F_y	Broken	
yz-plane	C_y	F_x	1245.3 Hz	20.2
yz-plane	C_z	F_x	1149.2 Hz	17.5

Table 26: Resonance frequency and Q-factor of Objet printed cantilevers.

Table 27 presents the resonance frequencies and the Q-factor of the measured cantilevers from DLP. It's seen that the resonance frequencies and Q-factors are lower compared to the Objet structures. This will be the result of a lower stiffness and a higher damping, respectively.

	Cantilever direction	Motion direction	Resonance freq	Q
xy-plane	C_y	F_z	1212.4 Hz	3.9
xz-plane	C_x	F_y	941.4 Hz	4.0
yz-plane	C_z	F_x	746.9 Hz	3.5

Table 27: Resonance frequency and Q-factor of DLP printed cantilevers.

The calculated Young's Modulus and standard deviation of the Objet structures are presented in table 28. The error analysis is of great importance in order to draw conclusions between different directions. The standard deviation $\Delta E/E$ of the Youngs Modulus is low (max 0.06). Therefore it is possible to draw some conclusions about the anisotropy in the material. It is seen that the cantilevers in the xy-plane display the highest stiffness. The cantilever in the z-direction show the lowest stiffness. These results indicate the existence of anisotropy in Young's modulus in the material.

	Cantilever direction	Motion direction	E (GPa)	$\Delta E/E$
xy-plane	C_x	F_z	2.5	0.06
xy-plane	C_y	F_z	2.5	0.06
xz-plane	C_x	F_y	1.6	0.06
xz-plane	C_z	F_y	Broken	
yz-plane	C_y	F_x	1.6	0.06
yz-plane	C_z	F_x	1.3	0.06

Table 28: Young's modulus of Objet printed cantilevers.

The Young's Modulus of the DLP printed structures are presented in table 29. Also for DLP there are clear indication of anisotropy in the Young's modulus

of the printed structures. Again the cantilevers in the xy-plane have the highest stiffness and the cantilever in the z-direction the lowest. The DLP structures are relative flexible compared with the Objet structures according to the lower Young's Modulus.

	Cantilever direction	Motion direction	E (GPa)	$\Delta E/E$
xy-plane	C_y	F_z	1.1	0.06
xz-plane	C_x	F_y	0.86	0.06
yz-plane	C_z	F_x	0.55	0.06

Table 29: Young's Modulus of DLP printed cantilevers.

5.2 Static Young's Modulus results

5.2.1 Measurement setup stiffness

First the stiffness of the measurement setup was measured, because a compensation has to be made for the deflection of the setup. Figure 33 presents the stiffness measured. The stiffness was measured left, middle and right on the weighing unit. A straight line is drawn between the three curves to estimate K_{op} of the setup. Table 30 indicates the calculated stiffness of the measurement setup.

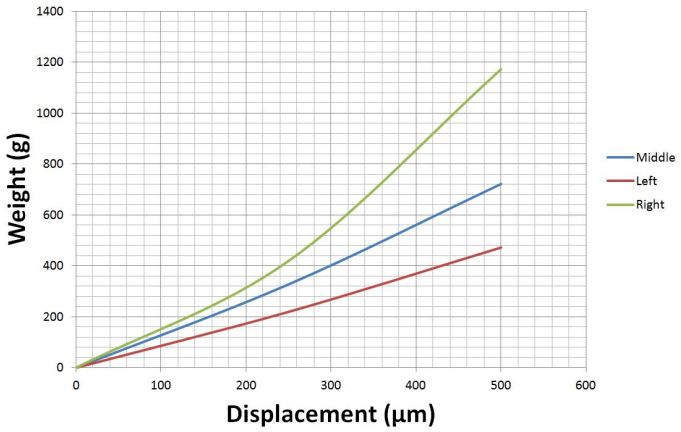

Figure 33: Stiffness of the test equipment, K_{op}.

Measurement setup stiffness	
K_{op} minimum	$7.8{\cdot}10^3$ N/m
K_{op} average	$1.2{\cdot}10^4$ N/m
K_{op} maximum	$1.6{\cdot}10^4$ N/m

Table 30: K_{op} of measurement setup.

5.2.2 Young's Modulus results

The displacement versus the weight was measured. The maximum displacement doesn't exceeded 1 mm in order to stay safe (no plastic deformation). Figure 34 represents the displacement versus weight of the total measurement system with Objet printed cantilevers. The slope of these lines represents the total stiffness, K_{eq}. The stiffness of the cantilever, K_{c} can be calculated in order to estimate the Young's Modulus.

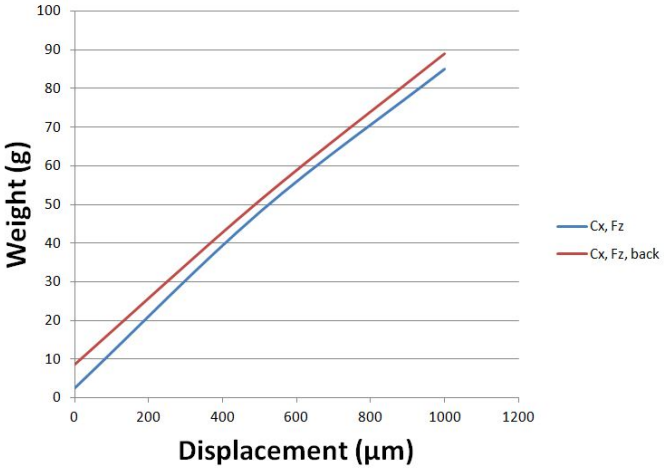

Figure 34: Total stiffness, K_{eq} with Objet cantilever C_x, F_z.

Table 31 presents the Young's Modulus and standard deviation of the measured Objet cantilevers. It's remarkable that the results from the static measurements differ from the dynamic measurements, but it is explainable because the error in the static measurements are relatively high. This is because many errors can be made during the measurements. All those errors together add up to a large deviation. Therefore those results are only indicative and no real quantitative conclusions can be drawn.

	Cantilever direction	Force direction	E (GPa)	$\Delta E/E$
xy-plane	C_x	F_z	2.5	0.28
xy-plane	C_x	F_z	2.2	0.27
xy-plane	C_y	F_z	1.7	0.35
xy-plane	C_y	F_z	1.8	0.33
xz-plane	C_x	F_y	0.98	0.68
xz-plane	C_x	F_y	1.0	0.69
xz-plane	C_z	F_y	0.86	0.90
xz-plane	C_z	F_y	Broken	-
yz-plane	C_y	F_x	1.1	0.61
yz-plane	C_y	F_x	1.1	0.28
yz-plane	C_z	F_x	Broken	-
yz-plane	C_z	F_x	Broken	-

Table 31: Young's Modulus of Objet cantilevers derived from static measurements.

Table 32 represents the Young's Modulus and standard deviation of the DLP cantilevers. Again the results of the static measurements differ from the dynamic measurements, this is explainable due to the large error in the static DLP measurement. It's remakable that the cantilevers C_x, F_z are very flexible (low E), even the most flexible of the measurement. This result is not inline with the dynamic results of the same direction and applied force, because the C_x, F_z cantilevers of the dynamic measurement were the stiffest. An explanation for this flexibility could be that during the removing of the designed supports the cantilevers were damaged.

	Cantilever direction	Motion direction	E (GPa)	$\Delta E/E$
xy-plane	C_x	F_z	0.16	0.74
xz-plane	C_z	F_y	0.48	0.32
yz-plane	C_y	F_x	0.39	0.38
xy-plane	C_x	F_z	0.13	0.84
xz-plane	C_z	F_y	0.47	0.32
yz-plane	C_y	F_x	0.28	0.45

Table 32: Young's modulus of DLP printed cantilevers derived form static measurements.

5.3 Equation verification measurement

The verification measurement was executed for one cantilever, the displacement, Δx was held constant at 500μm and the reaction force was measured at different lengths of the cantilever. Figure 35 represents the cantilever of DLP C_{x}, F_{z1} measured, and the calculated equation 10. $1/l^3$ is plotted versus the Force. However it was not possible to measure all cantilevers, because it was beyond the scope of the project.

$$F = \frac{3EI\Delta x}{l^3} = \frac{1.3933 * 10^{-7}}{l^3} \tag{10}$$

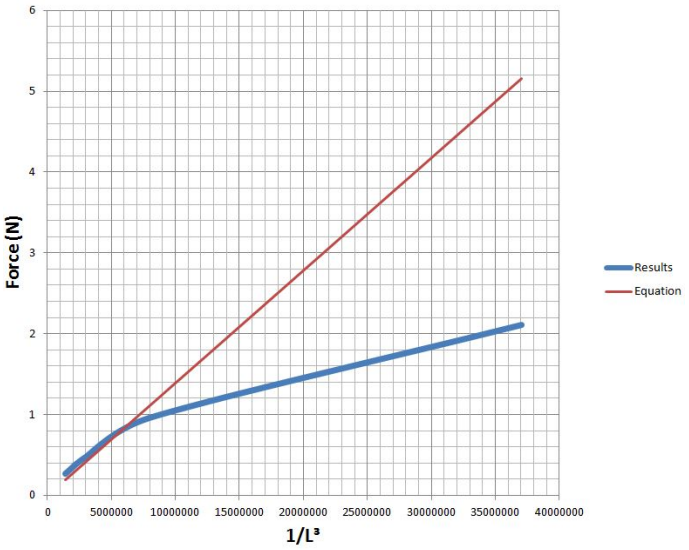

Figure 35: Verification.

The equation is linear, because $1/l^3$ is plotted. However the measured cantilever is not. The two lines should have the same slope. This is only the case for large L.

5.4 Conclusion Young's Modulus measurements

Two measurements methods were executed, the dynamic measurement and the static measurement in order to calculate the Young's Modulus. It is seen that the dynamic method was the most accurate method in order to estimate the Young's Modulus. The maximal standard deviation $\Delta E/E$ of the dynamic method was 0.06, this accurate method will give space to draw quantitative conclusions. It was seen that cantilevers in the xy-plane achieved the highest stiffness: C_x, F_z 2.5 GPa. The z-direction is the most flexible direction, with

1.3 GPa for the Objet cantilevers (table 28). These results show the anisotropy of the material. The results showed five broken cantilevers in the C_z direction, this might indicate that the tensile strength in the z direction is lower. It is important to take this into account during designing.

Also for the DLP structures there exist anisotropy with the stiffest in the xy-plane, C_y, F_z 1.1 GPa and weakest in the z-direction, C_z, F_x 0.6 GPa. These results indicates the difference between the Objet and DLP structures. It is seen that the DLP printed objects are the more flexible structures.

The results of the static measurements are only indicative, because the errors made during the measurements are far too big to draw any quantitative conclusions.

6 Shear Modulus results

6.1 Shear Modulus results of Objet and DLP

The measured Shear Modulus of the six possible orientations of the Objet structures are tabulated in table 33. The force acts on the xy, xz and yz-planes (area A of figure 19), with the directions $F_{x,y,z}$. The results lay between 0.20 GPa and 0.24 GPa. The deviation between the results isn't much higher than the standard deviation of the Shear Modulus, therefore it is not possible to draw any conclusions about possible anisotropy. The Shear modulus between different directions should be considered closely the same.

	Direction of Force	Shear Modulus (GPa)	$\Delta G/G$
xy-plane	F_x	0.24	0.08
xy-plane	F_y	0.23	0.07
xz-plane	F_x	0.22	0.07
xz-plane	F_z	0.21	0.07
yz-plane	F_y	0.20	0.07
yz-plane	F_z	0.23	0.07

Table 33: Shear Modulus and standard deviation of Objet structures.

The measured Shear Modulus of different orientations of DLP printed structures are presented in table 34. The deviation between the orientations are larger compared to the Objet structures, but it is not possible to draw any conclusion, because the printed structures deviated (small cracks and fractures) and it was not able to take the deviations into account into the error analysis. Also the values of the Shear Modulus are smaller compared to the Objet structures. This was already expected, because the Young's Modulus was also lower.

	Direction of Force	Shear Modulus (MPa)	$\Delta G/G$
xy-plane	F_x	12	0.08
xz-plane	F_x	8.6	0.06
yz-plane	F_z	12	0.08

Table 34: Shear Modulus and standard deviation of DLP structures.

6.2 Creep analysis

The last step of the analysis is focused on the creep of the structures. Two different loads were applied at two different shear structures in order to measure possible creep. Figure 36 indicates the displacement L due to two different loads applied. 4.489 Kg was applied for 30 minutes, after a few minutes the structure stabilised and no more displacement was measured. The structure didn't stabilise when 7.476 Kg was applied, the creep continues and after 30 minutes the test was stopped in order to prevent breaking of the structure.

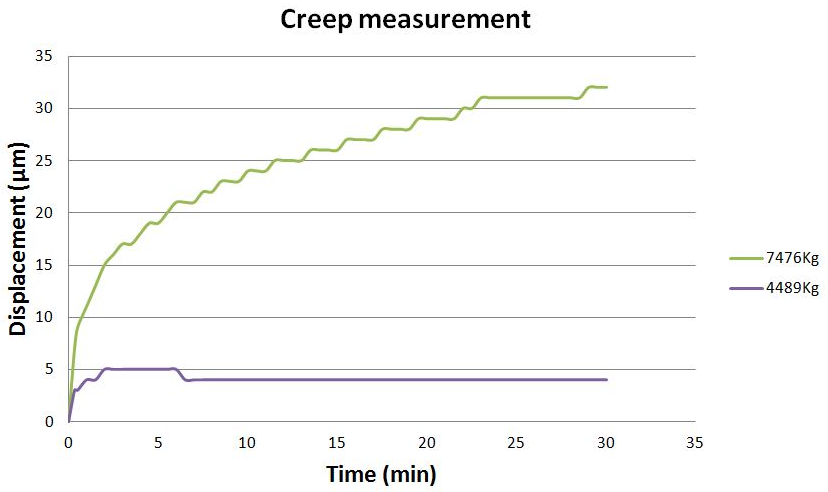

Figure 36: Creep due to shear tension.

6.3 Shear results conclusions

It was possible to measure the Shear Modulus without large deviations. The highest Shear Modulus was 2.4 GPa for the Objet structures table 33 and 12 MPa for the DLP structures (table 34). It can be concluded that the Objet structures have a lower response to shear stress compared to the DLP structures. Any anisotropy in the different directions couldn't be concluded, because the Shear Modulus deviations are closely the same compared to the standard deviations

of G. With the Shear Modulus and Young's Modulus known it should be able to determine the Poisson's ratio, However we are dealing with an anisotropic material and calculating the Poisson's ratio isn't so obvious.

7 Final conclusion

It was possible to measure all quantities. Only the dynamic and static Young's Modulus results were not inline, which has been attributed to a large error made in the static measurement. The minimum block sizes range between 150 μm and 500 μm for DLP and 250 μm and 300 μm for Objet structures. The accuracy achieved for the DLP was the best in the xy-plane, but worse in the other planes because no support is used which will results in bended beams. The accuracy for the Objet was on all planes approximately the same due to the support material. The support material increases the accuracy but has also an effect on the surface roughness and minimum block and hole size, those quantities were bigger compared to the DLP printed, because the support material has to be removed manually. The Young's Modulus and Shear Modulus of the Objet where max 2.5$\pm$0.15 GPa and 0.24$\pm$0.018 GPa and for the DLP 1.1$\pm$0.06 GPa and 12$\pm$0.1 MPa. Also their exist some anisotropy in the material; the Young's Modulus was highest in the xy-plane and smallest in the z-direction. With the mechanical properties known it is able to build real transducers. The minimum block size and accuracy are still high compared to MEMS technology, however it is possible to build transducers at an bigger size, furthermore it is possible to increase the manufacturing process of transducers with 3D print technology.

8 Bibliography

References

[1] 3d printing process. http://www.createitreal.com/index.php/technology/process, 2014.

[2] Binder jetting. https://www.additively.com/en/learn-about/binder-jetting,, 2014.

[3] binder jetting 3d printing. https://www.whiteclouds.com/3dpedia-index/binder-jetting-3d-printing,, 2014.

[4] Charles w. hull patent 'stereolithography'. http://www.google.com/patents/US4575330, 2014.

[5] Digital light processing principle. http://www.zspotmedia.ro/blog/noutati/printare-3d/, 2014.

[6] Dlp printer. http://brillianttechnology.nl/2011/04/07/perfactory-minixl-3d-dlp-printer,, 2014.

[7] The engineering toolbox. http://www.engineeringtoolbox.com/young-modulus-d, 2014.

[8] Fdm principle. http://www.custompartnet.com/wu/fused-deposition-modeling, 2014.

[9] Laminated object manufacturing. http://en.wikipedia.org/wiki/Laminated-object-manufacturing ,, 2014.

[10] Miicraft printer. http://www.miicraft.com/products/, 2014.

[11] Objet eden350. http://www.stratasys.com/3d-printers/design-series/precision/objet-eden350v,, 2014.

[12] Photopolymer. http://en.wikipedia.org/wiki/Photopolymer,, 2014.

[13] Principle of binder jetting, 2014.

[14] Principle of curl. http://www.emeraldinsight.com/journals.htm?articleid=1455136, 2014.

[15] Principle of lom, 2014.

[16] Principle of objet. http://www.hellopro.co.uk/Objet-Geometries-2951-noprofil-1001325-14800-0-1-1-fr-societe.html, 2014.

[17] Principle of selective laser sintering. https://www.flickr.com/photos/organ-printer/878476066, 2014.

[18] Shear modulus principle. http://en.wikipedia.org/wiki/Shear-modulus, 2014.

[19] Solid works. http://en.wikipedia.org/wiki/SolidWorks, 2014.

[20] Stereolithography principle. http://www.princeton.edu/ cml/html/research/mems.html, 2014.

[21] J. Kotlinski A. Kesy. *Mechanical properties of parts produced by using polymer jetting technology.* 2013.

[22] Pulak M Pandey N. Raghunath. *Improving accuracy through shrinkage modelling by using Taguchi method in selective laser sintering.* page 993, 2013.

[23] J. I. Craig O. A. Bauchau. *Euler-Bernoulli beam theory.* page 174, 2009.

[24] K. G. Swift. *Manufacturing process selection handbook.* page 241, 2013.